Constitutive constants for hot working of steels: the critical strain for dynamic recrystallisation in C-Mn steels

C W Siyasiya and W E Stumpf
Department of Materials Science and Metallurgical Engineering, University of Pretoria, South Africa
Corresponding author: charles.siyasiya@up.ac.za

Abstract

The primary focus of this work was to determine the relationship between chemical composition and the Zener-Hollomon exponent q in the peak strain equation for hot working of C-Mn steels with the ultimate aim of improving the modelling of mean flow stresses (MFS) for hot strip mills. Therefore, the hot deformation behaviour of C-Mn steels was examined in which the C and Mn contents were increased systematically between the levels 0.035 up to 0.52%C and 0.22 to 1.58%Mn respectively. In addition, data from other workers were also analysed to complement the results from this investigation. As opposed to the observations from some other workers that the apparent activation energy for hot working Q_{HW} appears to decrease with an increase in the carbon content, it was found that, despite a weak relationship, Q_{HW} increases with an increase in carbon content *i.e.* from 300 to 355 kJ/mol as was also found by others. Consequently, the Zener-Hollomon exponent q in the peak strain equation for hot working and hence also the critical strain for dynamic recrystallisation (DRX), $\varepsilon_c = 0.65AD_o^{\ m}Z^q$, was found to decrease with an increase in carbon content as follows, $q = 0.21 - 14[\%C]$ for $C \leq 0.8\%C$. The possible role played by Manganese-Carbon complexes in the austenite during hot working and the consequences of the variation in q for Compact Strip Production (CSP) rolling are discussed.

Keywords: dynamic recrystallization, Zener-Hollomon exponent, critical strain, Mn-C complexes

1. Introduction

1.1 Influence of carbon content on the apparent activation energy for hot working Q_{HW}

The disagreement on the effect of the carbon content on the Q_{HW} in plain C-Mn steels [1-4] during hot working has been addressed by various researchers [5-11]. Some studies have shown that increasing the carbon content promotes dynamic softening by an enhancement of the self-diffusion rate of iron through the reduction in the Q_{HW} [9-15]. However, the enhancement of dynamic softening is dependent on temperature and strain rate and Jaipal et al [10] observed that at low Zener-Hollomon parameters (Z, s^{-1}), *i.e.* at high temperatures and low strain rates, an increase in carbon content lowers the critical strain ε_c required for the onset of DRX and that at high Z values, carbon only increases the work hardening rate $\theta = d\sigma/d\varepsilon$. Collinson et al [5-7] also made similar observations of complex effects of carbon on the strength of austenite during hot rolling whereby increasing the carbon content lowered the flow stress by 30% at low Z values but increased it again by about 100% at high Z values. However, the mechanisms responsible for this behaviour were not explained.

The apparent activation energy for hot working, Q_{HW}, has been found by various authors to decrease with an increase in carbon content as follows [13]:

$$Q_{HW} = 318 - 93.43[C] \qquad (C<0.8\%) \tag{1}$$

and [14]:

$$Q_{HW} = 320 - 138.9[C_{eq}] \ (C_{eq} = C + Mn/6 \leq 0.35\%) \tag{2a}$$
$$Q_{HW} = 271 \qquad (C_{eq} = C + Mn/6 > 0.35\%) \tag{2b}$$

where C_{eq} is the carbon equivalent.

Medina et al [15] observed that Q_{HW} is not only influenced by the carbon content alone but by other alloying elements as well which generally increase it:

$$Q_{HW} = 276–2.535[C]+1.01[Mn]+33.62[Si]+35.65[Mo]+93.68[Ti]+31.673[V]+70.73[Nb] \quad (3)$$

Contrary to the observations above, Colàs, by using data from various workers, observed that Q_{HW} increases with an increase in carbon, manganese and silicon content as follows [16]:

$$Q_{HW} = 282.7 + 92.4[C] + 6.57[Mn] + [Si] \quad (4)$$

where Q_{HW} is in kJ.mol^{-1}, and all alloying elements are in mass %

Likewise, Crowther et al [17] made a similar observation that Q_{HW} increases with an increase in carbon content.

Furthermore, Gjostein et al [18] established that in plain carbon steels, the grain boundary energy γ_{gb} decreases with an increase in carbon content due to the increased carbon segregation to the grain boundaries and can be estimated using the following expression:

$$\gamma_{gb} = (0.8 – 0.35C^{0.68}) \quad (\text{in J.m}^{-2}) \quad (5)$$

where C is the carbon content in mass % with C ≤ 0.8%.

This implies that increasing the carbon content would lead to delayed DRX due to the decrease in grain boundary surface energy. In other words, this may lead to the retardation of the grain boundary migration rate or mobility by decreasing the effective driving force hence a higher Q_{HW}.

1.2. Constitutive equations for the steady state flow stress and the peak strain

There are two primary equations that are used to model the hot deformation behaviour of a metal under steady state deformation conditions [19,20]:

$$Z = \dot{\varepsilon} \exp\left(\frac{Q_{HW}}{RT}\right) = A_1[\sinh(\alpha\sigma_{ss})]^n \quad (6)$$

$$\varepsilon_p = A_2(D_0)^m Z^q \quad (7a)$$

Rewriting this equation yields:

$$q = \frac{\ln\left(\frac{\varepsilon_p}{A_2(D_o)^m}\right)}{\ln(\dot{\varepsilon}) + \left(\frac{Q_{HW}}{RT}\right)} \quad (7b)$$

where $\dot{\varepsilon}$ is the strain rate in s^{-1}, Q_{HW}, Z, R and T have their usual meanings, A_1, A_2 and α are material constants, σ_{ss} is the steady state flow stress in MPa, D_0 is the initial grain size in μm. The dimensionless constants n, m and q are considered to be constant with temperature. Note that in most steels the critical strain for the onset of DRX ε_c is a fraction of the peak strain $(0.65 \text{ to } 0.8)\varepsilon_p$ [19].

As may be seen from equation 7b above, an increase in either Q_{HW} or structural factor $A_2(D_o)^m$ or both will lead to a lower q value. If the Zener-Hollomon exponent q can be modelled by finding the relationship between q and $A_2(D_o)^m$ and Q_{HW} then the problem of deciding what q value to use in equation 7a, given the chemical composition of the steel, will be solved for estimating the onset of DRX for these plain C-Mn steels. Sellars [32] attempted to draw a relationship between q and the chemical

composition on data from other workers but could not observe an apparent systematic trend. Since the data was only from other workers the hot working test might not have been carried out systematically.

2. Experimental procedure

2.1 Hot compression tests

The nine steels given in Table 1 were subjected to single pass hot compression tests using the Gleeble 1500D^{TM} thermomechanical processing simulator with specially designed "isothermal anvils" to minimise temperature gradients. The samples were machined into cylindrical specimens 10 mm diameter and 15 mm long and the samples were soaked at 1150°C for 10 minutes and thereafter cooled to the deformation temperature at 10°C/s. The deformation temperature was varied between 900 and 1140°C while strain rates varied between 0.001 and $5s^{-1}$. Total true strains were limited to 0.8 or less to maintain the barrelling coefficient [21] to below 0.9. The true stress and true strain curves were calculated from the digital logged data and the flow stress was corrected to a Von Mises flow stress with correction for a friction coefficient of 0.1 [22] between the specimen and the tantalum foil placed between the WC anvils and the specimen.

Table 1: *Chemical compositions in mass % of the steels*

Steel	A140	P1	P2	VC8	VC7	VC5	VC9	VC6	EN9
C	0.035	0.038	0.051	0.10	0.12	0.15	0.25	0.41	0.52
Mn	0.320	0.250	0.224	0.14	0.36	0.80	1.14	1.58	0.70
Si	0.001	0.020	0.014	0.17	0.16	0.30	0.24	0.15	0.25
Al	0.122	0.050	0.045	0.07	0.01	0.03	0.08	0.02	0.01
S (ppm)	120	2	140	10	40	20	10	30	140
P (ppm)	170	80	50	50	10	10	10	10	160
N (ppm)	32	104	65	-	-	80	-	-	110

2.2 Austenite grain size measurement

The starting austenite grain size D_0 was determined through a hyper-eutectoid carburisation method based on the standard McQuaid-Ehn test [23]. The undeformed specimens were placed in the furnace at the soaking temperature in order to avoid uncontrollable grain growth during the slow heat cycle of the furnace. After soaking for 10 minutes, the temperature was dropped rapidly to 910°C for carburisation with a CO/CO_2 mixture. The carburised specimens were ground, polished and etched with 4% Nital. The linear intercept method was employed according to ASTM E112-10 to measure the austenite grain size where the grain boundaries had been "decorated" by cementite. At least 150 intercepts were measured for each of the steels.

3. Experimental results

3.1. Measured initial grain size, D_o

Typical micrograph used for the determination of the D_0 is given in Figure 1. A summary of the measured grain sizes are given in Table 2.

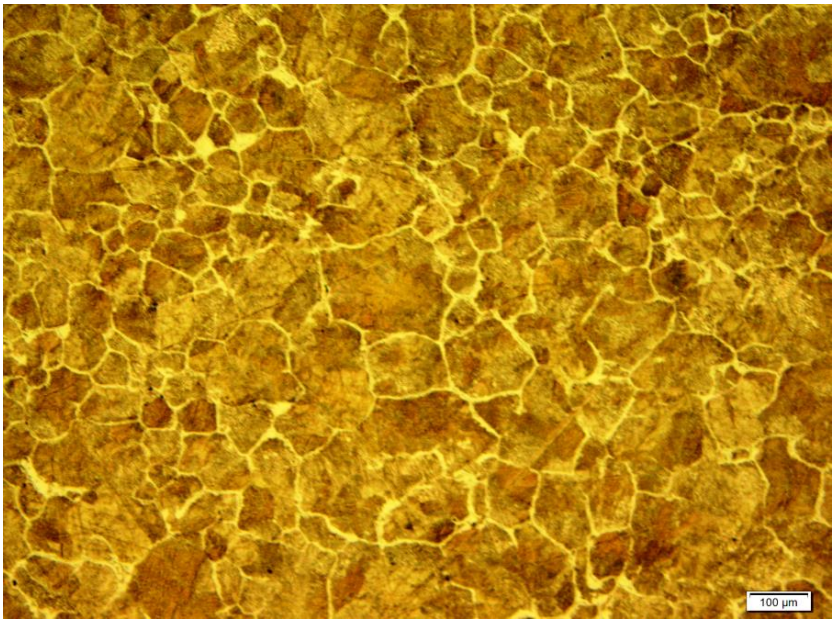

***Figure 1**: Typical austenite grain size after soaking at 1150°C for 10 minutes for one of the steels, VC5.*

***Table 2:** Measured grain sizes after the McQuid-Ehn test at 910°C*

Steel	VC8	VC9	P1	P1	P2	A140	A140	VC5	VC6	VC6	VC7	EN9
Temperature °C	1150	1150	1150	1200	1150	1150	1200	1150	1150	1200	1150	1150
D_0 (µm)	50	83	98	300	124	90	290	91	50	218	99	66

3.2. Apparent activation energy Q_{HW} for DRX for the various steels

Figure 2 shows the typical flow curves generated from the Von Mises corrected true stress versus true strain data. This is the data that were used to experimentally determine the Q_{HW} and q.

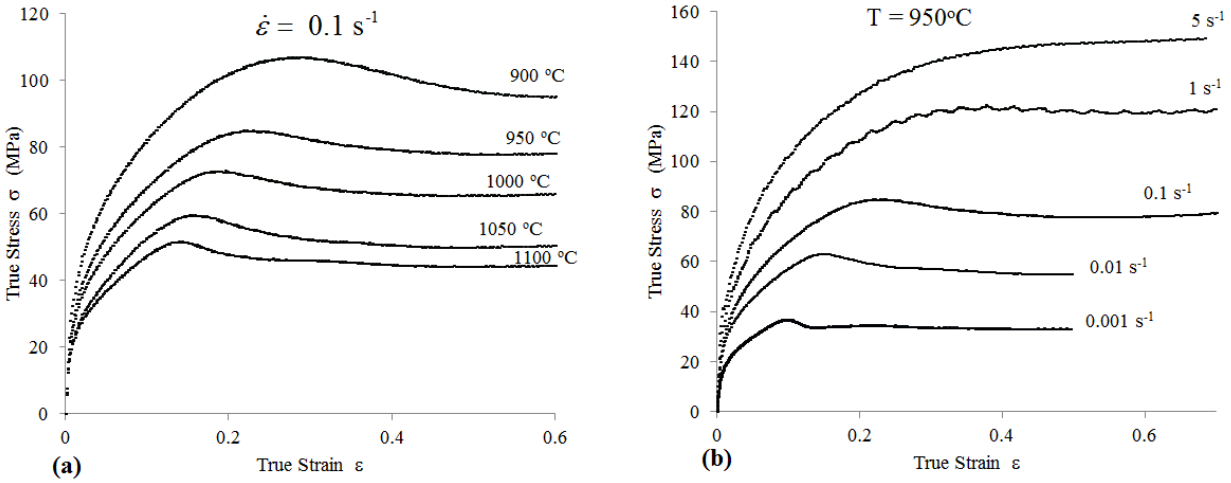

***Figure 2:** True stress versus true strain curves for Steel VC5 (a) strain rate of 0.1 s^{-1} but various temperatures (b) at 950°C but various strain rates.*

Figure 3 shows typical plots used to determine the constitutive constants for the hot working equation 6, namely Q, α, and n. The slopes of the plots in Figures 3(a) and (b), *i.e.* $\ln(\dot{\varepsilon})$ vs. $\ln(\sigma_{ss})$ and $\ln(\dot{\varepsilon})$ vs. σ_{ss} were used to determine the material constants n', and β respectively for the calculation of α. The slopes of the plots of $\ln(\sinh(\alpha\sigma_{ss}))$ vs. $(1000/T)$ and $\ln(Z)$ vs. $\ln[\sinh(\alpha\sigma_{ss})]$ in Figures 3(c) and (d) were used to determine the apparent activation energy Q_{HW} and n respectively.

Table 3 shows that the general trend is that Q_{HW} increases with an increase in the carbon content. Possible reasons for this behaviour are discussed in detail in section 4.1.

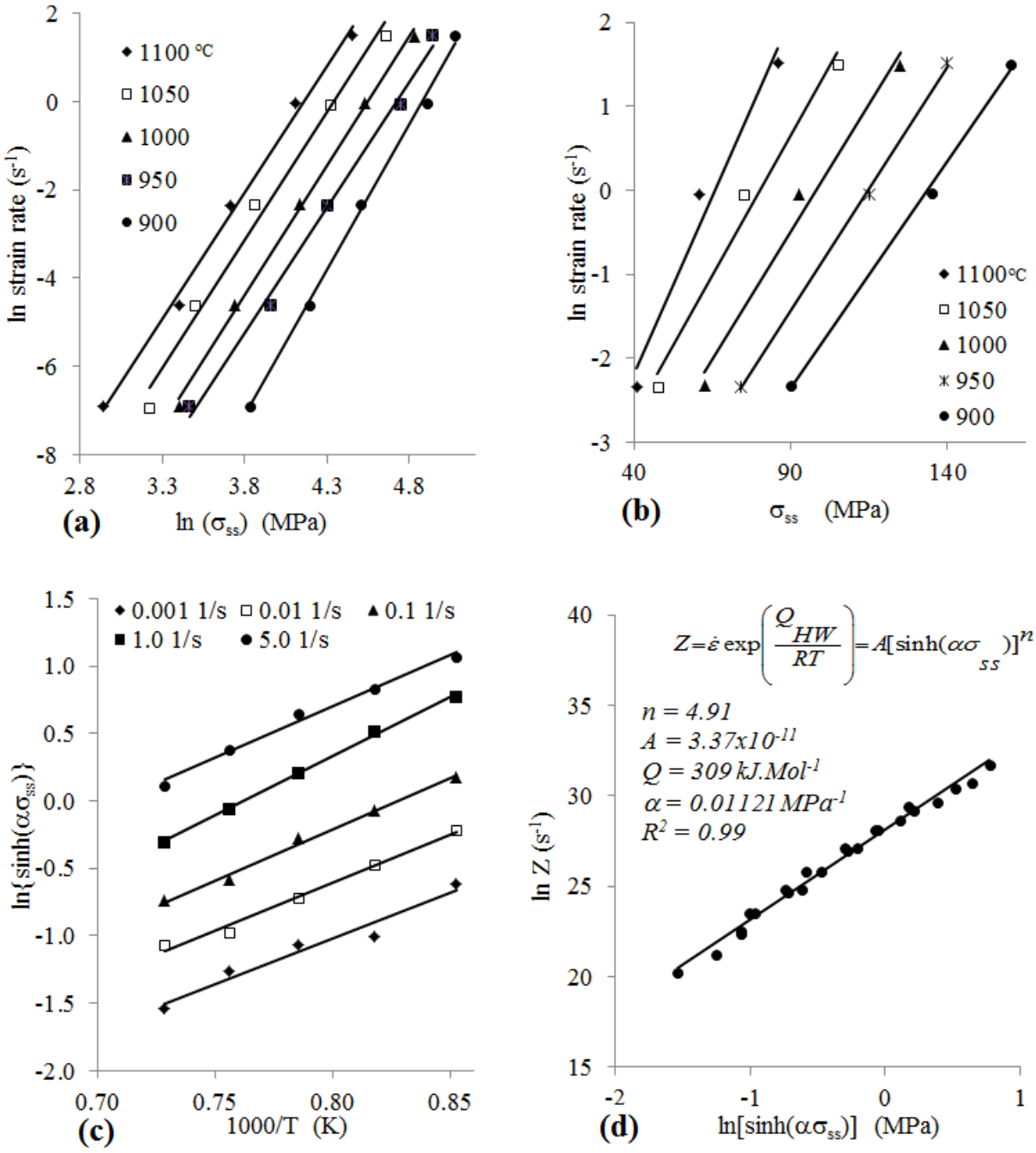

Figure 3: *Plots for steel VC5: (a) Plots of* $\ln(\dot{\varepsilon})$ *versus* $ln(\sigma_{ss})$ *and (b)* $\ln(\dot{\varepsilon})$ *versus* σ_{ss} *for determination of* n', *and* β *to calculate* α, *(c)* $ln(sinh(\alpha\,\sigma_{ss}))$ *vs. (1000/T) out of which an average of*

five values of the slope Q_{HW}/nR is obtained, (d) the slope after plotting all data of VC5 as ln(Z) versus ln(sinh($\alpha\ \sigma_{ss}$) provides the exponent n and the intercept A_1 in equation 5.

Table 3: *The hot working activation energy Q_{HW} as determined using the data in Figure 4*

Steel	P1	P2	A140	VC8	VC7	VC5	VC9	VC6	EN9
Mass %C	0.038	0.051	0.035	0.12	0.13	0.15	0.3	0.4	0.52
Q_{HW} (kJ.mol^{-1})	300	309	321	347	306	309	355	333	332
n	4.7	4	4.6	5.4	4.4	4.9	5.2	5.5	7
α (MPa^{-1})	0.0143	0.0143	0.0128	0.0115	0.0132	0.0112	0.0112	0.0110	0.0130
$A(D_o)^m$	0.0030	0.0011	0.0006	0.0010	0.0007	0.0013	0.0015	0.0025	0.0052

The apparent activation energy for hot working Q_{HW} for the steels investigated in this work as well as data from other workers [11,12,15,17,24-31] are plotted against the carbon content in Figure 4. Despite the scatter, the general trend is that Q_{HW} increases with an increase in carbon content of the steel. The scatter might be a result of varying test conditions.

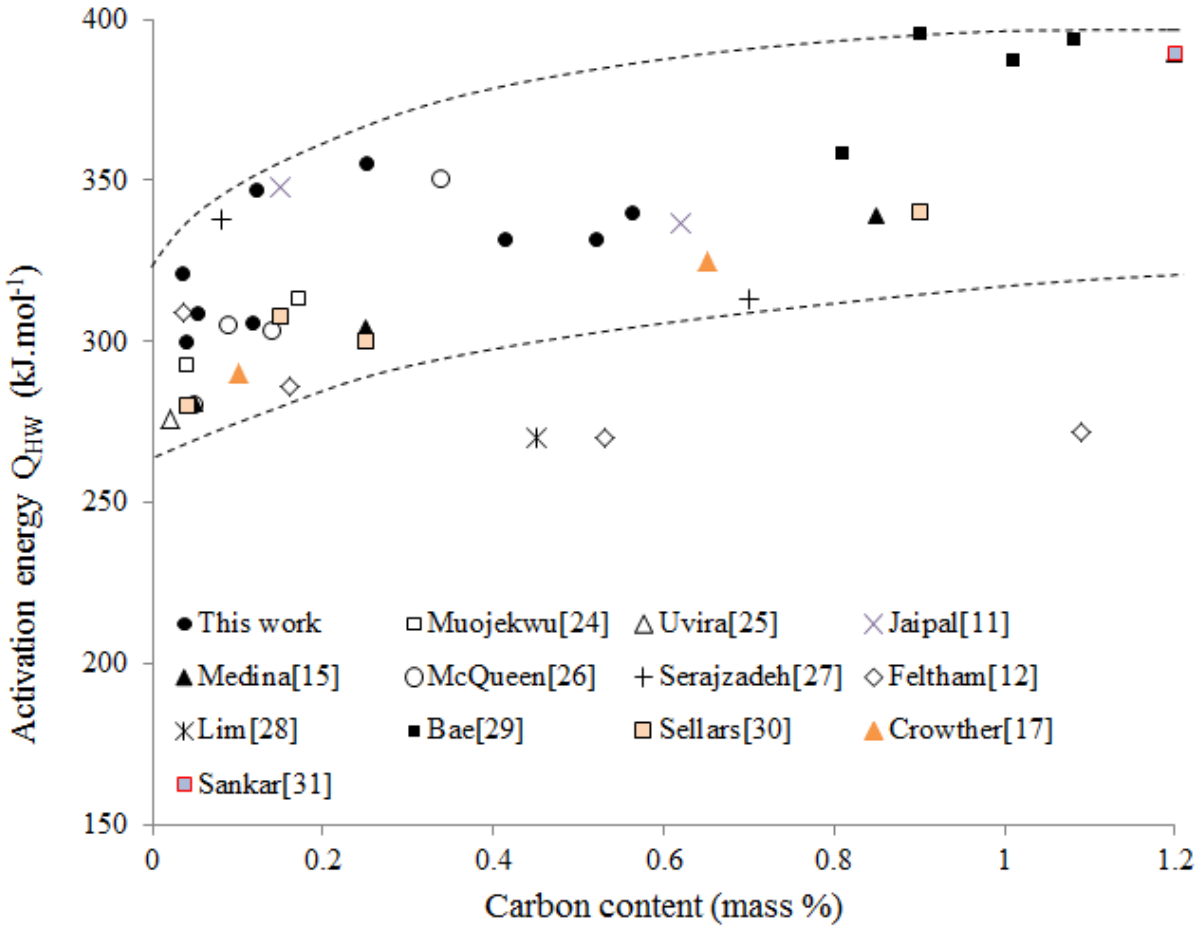

Figure 4: *Plot of the apparent activation energy for hot working Q_{HW} versus the carbon content of the various steels investigated in this work as well as data from other workers.*

3.3. The Zener-Hollomon exponent q in the peak strain equation

Equation 7a is plotted using experimental data from the steels which were investigated in this work in Figures 5a and b. The Z exponent q was found to be about 0.2 and 0.15 in low and medium C steels respectively. The structure factor A_2 for the peak strain equation 7a determined from this work as well as data from other researchers is plotted against the carbon content in Figure 6. Despite the scatter, A_2 increases with an increase in the carbon content of the steel. Possible reasons for this behaviour are discussed in section 4.1.

The $\ln(\varepsilon_p)$ is plotted against $\ln(Z)$ in Figures 7a and b. The soaking temperature was varied from 1150 to 1200°C in order to vary the initial grain size D_o and, as may be seen, q is not significantly influenced by the change in D_o in both steels *P1* and *A140*. Similar results were also obtained for steel *VC6* where q was found to be 0.16 and 0.15 for D_o of 218 and 50 µm respectively.

Values for q determined from this work together with data from other workers [15,27,29,31-34] are plotted against the carbon content in Figure 8. Despite some scatter, it is evident that q decreases with an increase in carbon content and somewhat levels off at about *0.08* beyond the eutectoid composition of these plain C and C-Mn steels, i.e.:

$$q = 0.21 - 14[\%C] \quad \text{for} \quad C \leq 0.8\%C \tag{8}$$

The outlier from Barraclough [34] was not from plain C or C-Mn steel but from an alloyed steel AISI 5140.

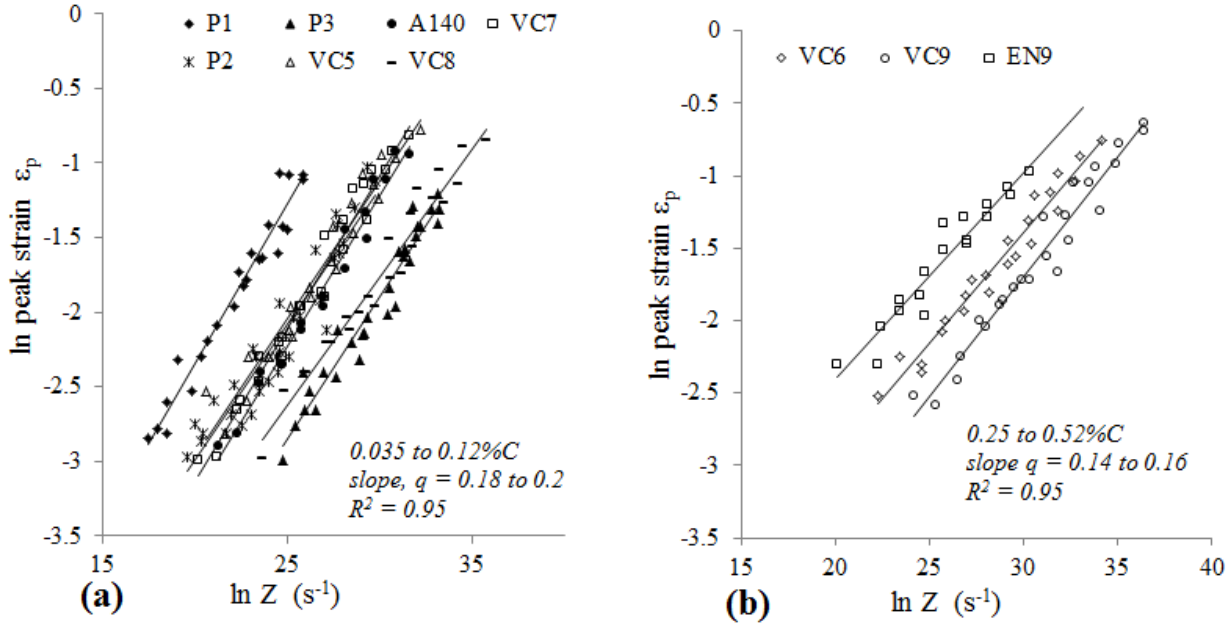

Figure 5: *Plots of the $\ln(\varepsilon_p)$ versus $\ln(Z)$ for the various steels after soaking at 1150 °C for 10 minutes and isothermally deformed between 900 and 1100 °C at strain rates between 0.001 and 5 s^{-1}, (a) low C and (b) medium C steels.*

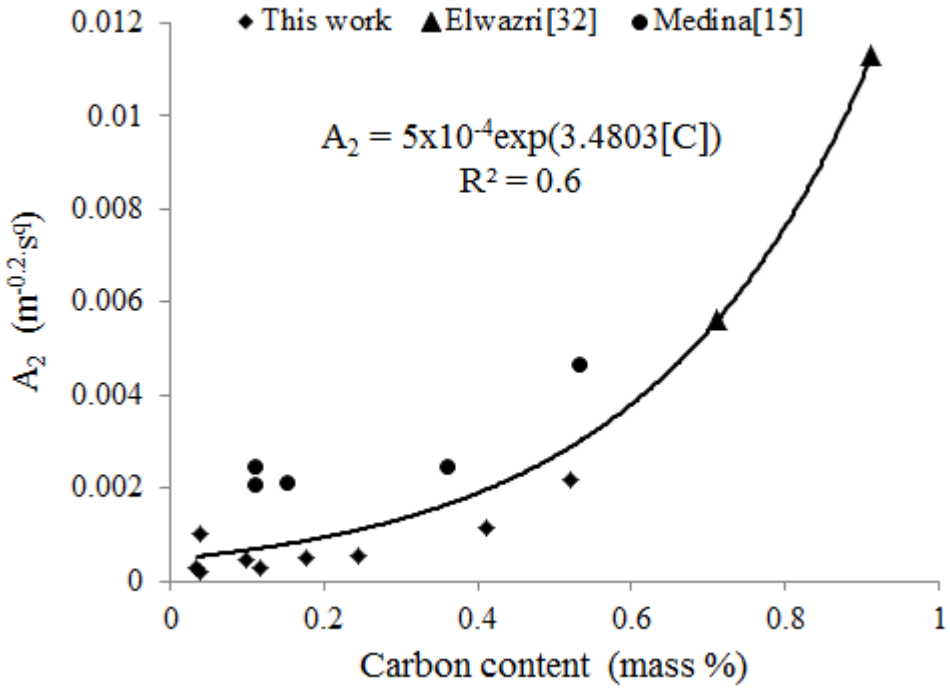

Figure 6: *Plot of the structural factor A_2 versus the carbon content in mass %.*

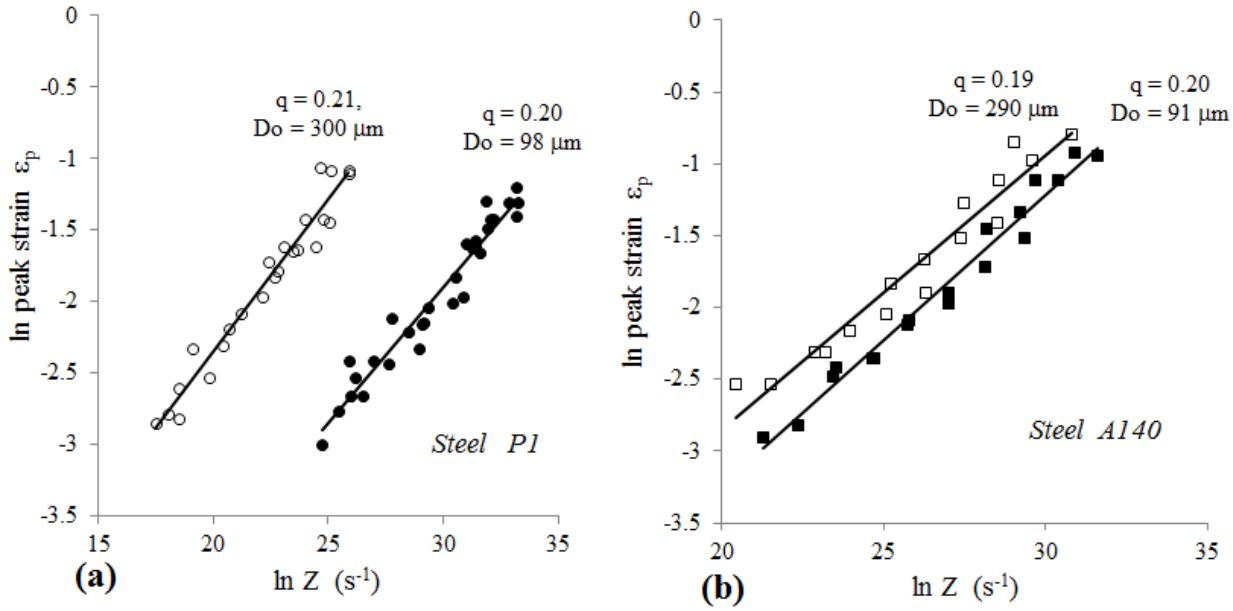

Figure 7: *Plots of $ln(\varepsilon_p)$ versus $ln(Z)$ for steels P1 and A140 in which D_o was varied by increasing the soaking temperature from 1150 to 1200°C for various times (a) steel P1 and (b) steel A140.*

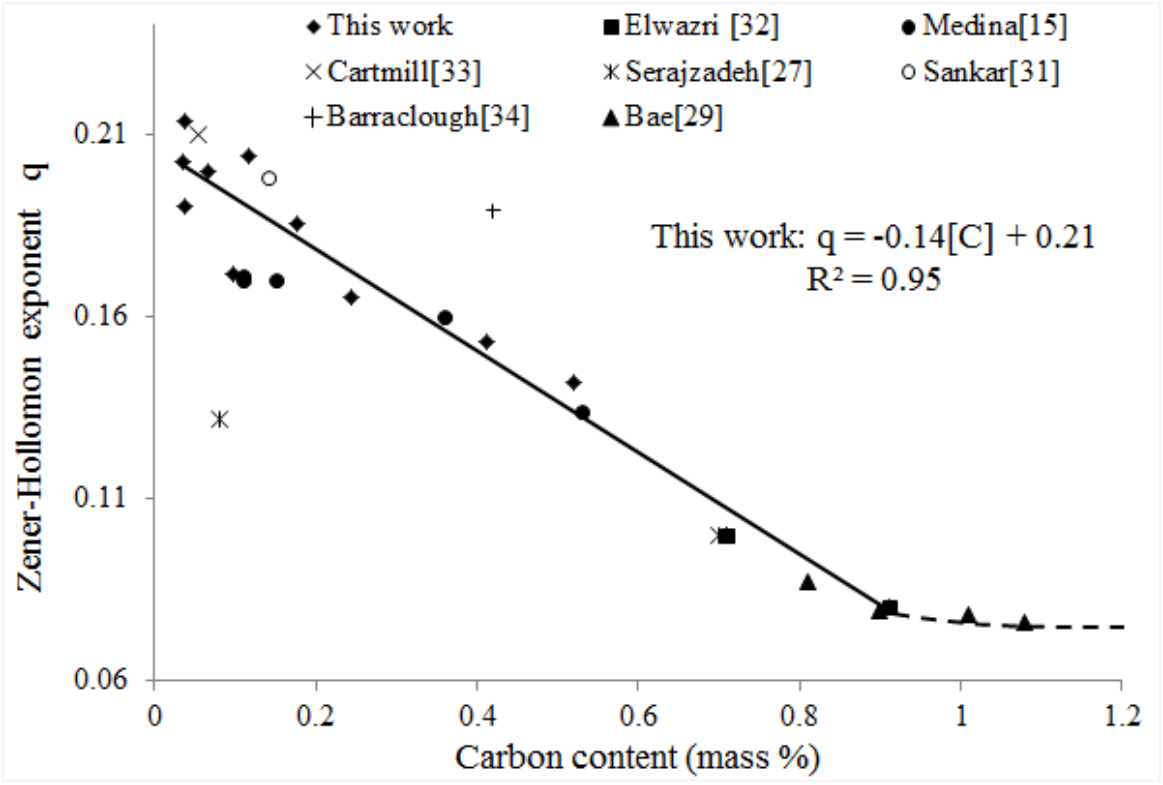

Figure 8: *Plot of* q *versus carbon content for this work as well data from others [15,27,29,31-34].*

4. Discussion

Equation 7b shows that q decreases with an increase in both the structural factor A_2 and the apparent activation energy for hot working Q_{HW}. Figures 4 and 6 show that both A_2 and Q_{HW} increase with an increase in the carbon content. Hence, q decreases with an increase in the carbon content from about 0.22 to 0.08 for low C and eutectoid steels respectively, see Figure 8. This is contrary to the observation made by Sellars [32] who, after plotting data from various workers with unspecified deformation conditions, found that q varied between 0.125 and 0.175 and that there was no apparent systematic relationship with chemical composition. In view of the observations made on C-Mn steels in this work, the role of C and Mn-C complexes have been explored in order to understand the relationship between q and chemical composition.

4.1. Interaction of Mn-C complexes with dislocations

The observation from this work that Q_{HW} increases with an increase in carbon content suggests that the effect of carbon in promoting dynamic softening (as a result of increased self-diffusion of iron from a strained matrix) , *i.e.* which should reduce the Q_{HW}, is overridden by other factors. Ushioda et al [33] found that in C-Mn steels it is the Mn-C complexes rather than manganese acting alone that suppresses the climb rate of dislocations and this was modelled by these authors in ferrite up to a temperature of 700°C. It is assumed that the climb rate of dislocations is determined by the vacancy flow to and from the dislocations and in pure metals the velocity of a climbing dislocation v_0 is given by [35]:

$$v_0 = \frac{D_{SD} b^2 2\pi}{kT \ln\left(\frac{R_d}{b}\right)}.\sigma \qquad (9)$$

where D_{SD} is the self-diffusion coefficient, b is the Burger's vector, R_d is the cut-off radius of the stress field of the dislocation, *i.e.* distance between dislocations and is estimated to be (~100b), σ is the applied stress, k and T have the usual meaning. Sandoström [36] modified equation (9) to take into account the effect of the substitutional atoms on the climbing rate of the dislocation and arrived at the following expression:

$$v = \frac{D_{SD} b^2 2\pi}{kT} . \frac{1}{\ln\left(\frac{R_d}{b}\right) + \left(\left(\frac{D_v^{III}}{D_v^{II}}\right) . \ln\left(\frac{r_1}{r_0}\right)\right)} . \sigma \qquad (10)$$

where D_v^{II} and D_v^{III} are the diffusion coefficients of vacancies in the region of the dislocation core as affected by the solvent and solute respectively, r_0 is the radius of the dislocation core *(~b)* and r_1 is the radius in the vicinity of the dislocation core *(~2b)*. The following equations were assumed by Sandström for D_v^{II} and D_v^{III}:

$$D_v^{III} = D_{SD}^{A} . C_v . v_a \qquad (11)$$

and

$$\frac{1}{D_v^{II}} = \frac{1}{D_v^{III}} + \frac{1}{D_{SD}^{B} . C_v . v_a . \exp\left(-\frac{\Delta E_{ie}}{kT}\right)} \qquad (12)$$

where C_v is the density of vacancies and the activation energy for formation of vacancies in FCC iron was assumed to be $\Delta H = 284$ kJ.mol^{-1}, v_a is the atomic volume b^3, D_{SD}^{A} and D_{SD}^{B} are the diffusion coefficients of A (solvent-Fe) and B (solute-Mn) atoms respectively and ΔE_{ie} is the interaction energy between the dislocation and the solute atom.

Table 4: *Parameters and constants used to evaluate the ratio v_0/v in FCC iron*

Parameter	Value	Ref
b (Burger's vector for FCC Fe)	2.60×10^{-10} (m)	
D_{SD}^{A}	$5 \times 10^{-5} \exp(-284000/RT)$ ($m^2.s^{-1}$)	37
D_{SD}^{B}	$1.6 \times 10^{-5} \exp(-261500/RT)$ ($m^2.s^{-1}$)	38
Atomic radius of Fe	1.24×10^{-10} (m)	
ΔE_{ie}	0.15eV (14.45 kJ/mol)	40

The ratio v_o/v between 900 and 1100°C was estimated from the above equations to range between 1.97 and 2.03 respectively meaning that the dislocation climb rate is about 2 times slower because of the presence of the Mn-C complexes. These two estimated values are somewhat close to each other as equation 10 does not take into account the fraction of the Mn-C complexes as the temperature and chemical composition vary. It is expected that the fraction of the Mn-C complexes may increase with an increase in C and Mn content [47]. Hence an increase in the structural factor A_2 may be expected with an increase in carbon content which is a result of the interaction of the dislocations with the Mn-C complexes. As expected, these ratios of v_o/v calculated for austenite from this work are lower than what Ushioda et al [33] found in similar steels in ferrite at lower temperatures ranging between 400 and 700°C whereby the respective dislocation climb rate ratios v_o/v were predicted to be between 17 and 5 times slower in the presence of Mn-C complexes. This difference between the estimates of this study and those of Ushioda et al [33] is not only temperature related but the difference in the binding energies between

the manganese and the carbon atoms, *i.e.* 0.46 eV in ferrite [39] versus 0.029 eV in austenite [41]. The local magnetic interaction somewhat increases the Mn-C-Fe binding energy in ferrite [42].

The fundamental influence of carbon on DRX in the binary FCC Fe–C system is different from that of the Fe-Mn-C system. In the former, the carbon is interstitial while in the latter it is attached to Mn as Mn-C complexes [41]. Hence, the two should not be treated the same way. In the binary FCC Fe–C system, it was found that the interstitial carbon atoms form interstitial-vacancy (*i*–vac) complexes [43,44]. However, no explanation could be found how these complexes increased the self-diffusion of iron except for the dilation of the matrix due to interstitial carbon atoms [45]. It was also shown that these *i*–vac complexes do not have a significant thermodynamic effect on the formation of mono-vacancies because of their inherently high enthalpy of formation [46]. If Mn is added to these steels, Mn-C complexes form readily and are responsible for the higher strain hardening rate in the austenite of C-Mn steels and their probability of forming increases with temperature [47].

4.2. The influence of chemical composition on the structural factor A_2.

It is evident from Figure 6 that the structural factor A_2 increases with an increase in the carbon content of the steel which implies that q will decrease with an increase in carbon content, see equation 7b and Figure 8. However, as may be seen from Figure 7, it would appear that q is not significantly influenced by D_o. This strongly suggests that the carbon atoms bound together with Mn atoms as Mn-C complexes, retard the dislocation movement and that grain size may not play a significant role in this mechanism at high strain rates experienced in rolling mills. Consequently, both A_2 and Q_{HW} increase with an increase in carbon content while q decreases with the latter, equation 7b.

4.3. Modelling the critical strain ε_c for dynamic softening of low versus medium C-Mn steels for a typical CSP rolling mill

The typical values of the nominal strain, the redundant strain, the forward slip factor and the strain rate per pass for a compact strip production (CSP) mill with typical reduction from a 75 mm slab to a 2 mm strip of a 0.04%C – 0.25%Mn steel at a hot strip mill in South Africa are given in Table 5 below. The critical strain ε_c for the initiation of dynamic softening was determined by plotting the second derivative of the 10th polynomial fit of the true stress-true strain curve against the ratio of stress over peak stress σ/σ_p . The average ratio of critical strain over peak strain $\varepsilon_c/\varepsilon_p$ for all of these steels was found to be 0.65 [48] and in agreement with Sellars [19]. The critical strain ε_c was calculated from the experimentally determined Q_{HW}, $A(D_o)^m$ and the predicted $q = 0.21 – 0.14[C]$ for the various hot rolling stands in a CSP rolling mill as shown in Table 5. The total strain per pass from mill log data and critical strain ε_c for the two selected low and medium plain carbon steels P2 and EN9 are plotted against the hot rolling stands in Figure 9 below.

It is evident from Figure 9 that the higher carbon steel EN9 (0.52C– 0.7Mn) may undergo dynamic softening from stands R1 to F3 whilst the lower C steel P2 (0.05C–0.22Mn) from the stands R1 to F2 *i.e.* for the same hot rolling conditions, the higher C steel EN9 experiences more dynamic softening that the lower C steel P2. Therefore, it may be concluded from Figure 9 that the low C steel undergoes dynamic recovery (DRV) in the last three finishing stands whilst the medium C steel probably only in the last two stands. Stumpf [49] made similar observations in a study on grain size modelling of low C strip steels where it was found that DRV takes place in the last three finishing stands of the CSP rolling mill. However, the study did not include medium C steels.

The difference in dynamic softening behaviour between low and high C steels is attributed to the increased self-diffusion of iron due to the straining effect of interstitial solid solution of carbon. However, this view does not take into account the interactions of Mn-C complexes with the dislocations as demonstrated in sections 4.1 above. It has been shown that both the Mn-C complexes may, to an extent, retard dislocation movement and, therefore, it is not surprising to observe more DRX in the higher C steel than in the lower C steel at the same pass in the hot strip mill. In austenite with a low SFE of about 20

$mJ.m^{-2}$ [50] the dominant softening mechanism is through climbing of dislocations rather than by cross slipping of dislocations. Therefore, it is expected that there would be less DRV in higher C steel due to lower mobility/climb rate of dislocations and as a result there would be more accumulated strain to induce DRX. Hence, more dynamic softening would occur in higher C steels.

The difference in the dynamic softening behaviour between low and high C steels is quite important for the design of the hot rolling schedules in terms of mill loads. In other words, these two categories of steels should not necessarily be hot rolled using the same schedule since the high C steel would be softer than the low C steel due to the extent of dynamic softening particularly in the finishing stands *i.e.* F3 versus F2 respectively for CSP rolling, see Figure 9. Inability to take into account this difference in DRX behaviour between these two grades of steels when determining the rolling schedules may result in mill instability [51].

Table 5: *Typical hot rolling parameters from the CSP rolling mill [52] and experimentally determined data used to determine the critical strain for initiation of DRX*

Steel	**Parameter**	**Roughing mill**		**Finishing mill**				
Process parameters	**Stand**	**R 1**	**R 2**	**F1**	**F2**	**F3**	**F4**	**F5**
	Effective strain rate (s^{-1})	7.7	17.5	18.9	46.6	73.4	118.4	147.6
	Total strain ε_T	0.87	0.79	0.94	0.8	0.48	0.39	0.3
	Temperature (^oC)	1106	1047	990	960	930	905	877
P2 (0.05C-0.22Mn)	Q_{HW} ($kJ.mol^{-1}$)	309	309	309	309	309	309	309
	$A(D_0)^m$	0.0011	0.0011	0.0011	0.0011	0.0011	0.0011	0.0011
	q = 0.21-0.14[C]	0.205	0.205	0.205	0.205	0.205	0.205	0.205
	predicted peak strain	*0.401*	*0.607*	*0.801*	*1.116*	*1.429*	*1.802*	*2.207*
	critical strain ($0.65\varepsilon_p$)	*0.261*	*0.395*	*0.520*	*0.725*	*0.929*	*1.172*	*1.435*
EN9 (0.52C-0.7Mn)	Q_{HW} ($kJ.mol^{-1}$)	332	332	332	332	332	332	332
	$A(D_0)^m$	0.0052	0.0052	0.0052	0.0052	0.0052	0.0052	0.0052
	q = 0.21-0.14[C]	0.137	0.137	0.137	0.137	0.137	0.137	0.137
	predicted peak strain	*0.37*	*0.49*	*0.60*	*0.76*	*0.90*	*1.06*	*1.22*
	critical strain ($0.65\varepsilon_p$)	*0.24*	*0.32*	*0.39*	*0.49*	*0.58*	*0.69*	*0.79*

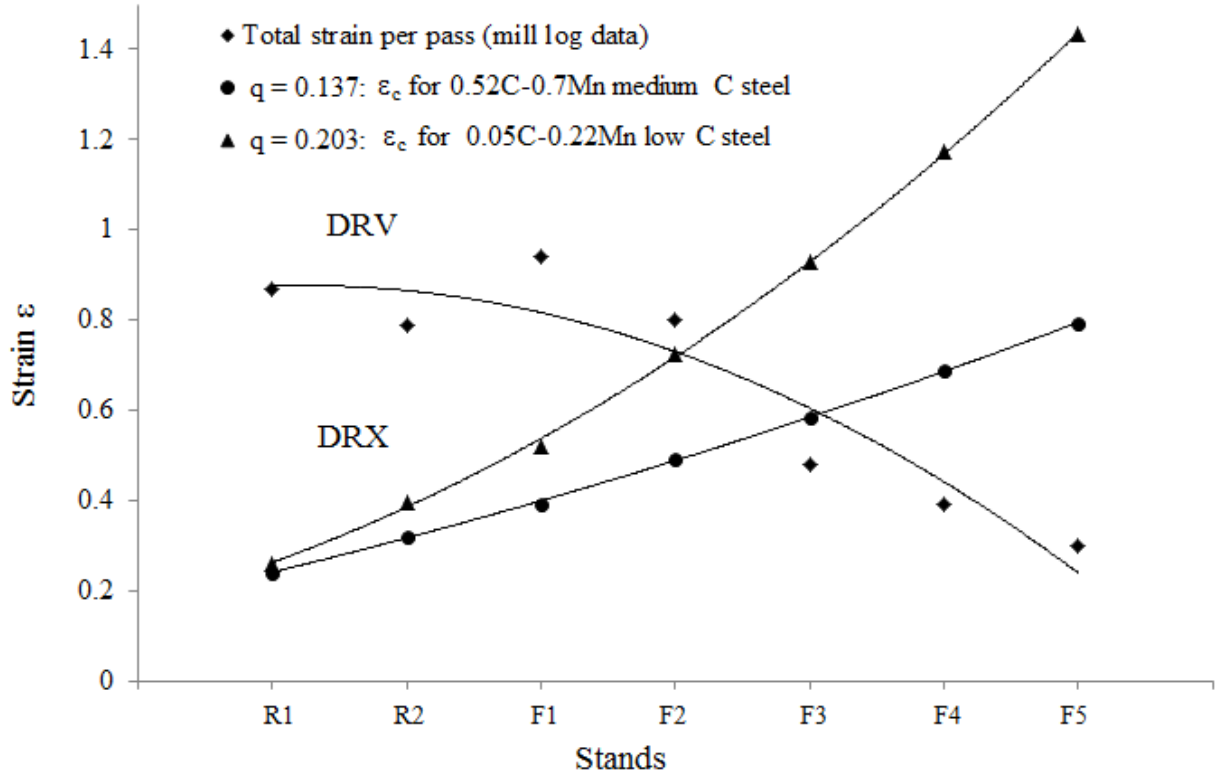

Figure 9: *Plots of total strain per pass from mill log data and the modelled critical strain* ε_c *for the initiation of DRX for the low and medium plain carbon steels P2 and EN9 respectively.*

5. Conclusions

The influence of chemical composition on the apparent activation energy of hot working and the Zener-Hollomon exponent q for the peak strain has been investigated in plain C-Mn steels and the following may be concluded:

- The apparent activation energy for hot working, $Q_{HW,}$ increases with an increase in carbon content in plain C-Mn steels, as was also found by others. Through estimated calculations, it has been shown that this is possibly due to the retarding effect that the Mn-C complexes have on the movement of dislocations.
- The exponent q in the equation for the critical strain to incur DRX has been found to decrease with an increase in A_2 and Q_{HW} (both of which increase with an increase in the carbon content), and also decreases with an increase in the carbon content according to $q = 0.21 – 0.14[C]$.
- Consequently, higher C steels undergo DRX preferentially as a result of less mobility of dislocations which limits DRV, *i.e.* enough strain is accumulated to induce DRX. The implication is that for a hot strip plant, low and medium C steels should ideally be rolled using different schedules in order to avoid mill instability.

6. Acknowledgement

The authors would like to acknowledge the financial support from the University of Pretoria through its Research Development Program and the use of its facilities. ArcelorMittal SA is also thanked for kindly providing some of the test materials and Dr Kevin Banks for his valuable contribution. Permission from the University of Pretoria to publish this work is also kindly acknowledged.

7. References

[1] T. Sakai and M. Ohashi, The effect of temperature, strain rate, and carbon content on hot deformation of carbon steels, Tetsu To Hagane, Vol. 67 No. 11, 1981, pp 134 – 143.

[2] C. Rossard et P. Blain, Recherches sur la deformation des aciers a chaud, IRSID, Series A, No. 174, 1957.

[3] P. J. Wray, Effect of composition and initial grain size on the dynamic recrystallization of austenite in plain carbon steels, Met. Trans. A Vol. 15A, 1984, pp 2009 – 2019.

[4] P. J. Wray, Effect of carbon content on the plastic flow of plain carbon steels at elevated temperatures, Met. Trans. A Vol. 13A, 1982, pp 125 – 134.

[5] D. C. Collinson, P. D. Hodgson and B A Paker, The deformation and recrystallization behaviour of austenite, Conf. Proc. on Modelling of Metal Rolling Processes (IOM), 1993, pp 283 – 295.

[6] D. C. Collinson, P. D. Hodgson and B. A. Paker, "The Deformation and Recystallisation. Behaviour of Austenite During Hot Rolling" Eds. J. J. Jonas, T. R. Bieler and K. J. Bowman, (TMS, Mass. 1993), pp 41 -58.

[7] D. C. Collinson, P. D. Hodgson, and C. H. J. Davies, The effect of carbon on the hot deformation and recrystallization of austenite, Themec'97, Wollongong, Australia, 1997.

[8] Y. Misaka and T. Yoshimoto, Japan Society for Technology of Plasticity, Formularization of Mean Resistance to Deformation of Plain. Carbon Steels at Elevated Temperature, Vol. 8 (1967), pp 414 – 442.

[9] S. Shida, Empirical Formula of Flow Stress of Carbon Steels - Resistance to Deformation of Carbon Steels at Elevated Temperature, Japan Society for Technology of Plasticity, Vol. 10, (1969), pp 610 – 617.

[10] T. J. Dixon, C. M. Sellars and J. A. Whiteman, The effect of carbon content during hot deformation of austenite, 37th MWSP Conf. Proc., ISS, Vol. XXXIII, 1996, pp 705 – 710.

[11] J. Jaipal, C. H J. Davies, B. P. Wynne, D. C. Collinson, A. Brownrigg, P. D. Hodgson, Effect of carbon content on the hot flow stress and dynamic recrystallization behaviour of plain carbon steels, Int. Conf. on Thermomechanical Processing of Steels & Other Materials, Eds. T. Chandra and T. Sakai, The Minerals, Metals & Materials Society, 1997.

[12] P Feltham, The plastic flow of iron and plain carbon steels above A_3 point, Proc. Phys. Soc: B66 (1953) pp 865.

[13] C. Nagasaki and J. Kihara, Tetsu-to-Hagane, ISIJ, The effect of carbon content on deformation resistance of carbon steels in the austenite temperature range, 1998, (in Japanese).

[14] T. Inoue, S. Nanba, M. Katsumata and G. Anan: Proc. Of Int. Conf. on Modelling of Hot Rolling, ed. By S Yue, CIM, Quebec, (1990), pp 290.

[15] S. F Medina and C. A. Hernandez, General expression of the Zener-Hollon parameter as a function of the chemical composition of low alloy and microalloyed steels, Acta Mater. Vol. 44, No. 1, 1996, pp. 137 – 148.

[16] R. Colàs, J. A model for the hot deformation of low carbon steel, Materials Processing Technology, 62, 1996, pp. 180 – 184.

[17] D. N. Crowther and B. Mintz, Influence of carbon on hot ductility of steels, Materials Science and Technology, Vol. 2 (1986), 671 – 676.

[18] N. A. Gjostein, H. A. Domain, H. I. Aaronson and E. Eichen: Relative interfacial energies in Fe-C alloys, Acta Metall., 1966, Vol. 14, pp. 1637 – 1644.

[19] C. M. Sellars, and J. A. Whiteman, Recrystallization and grain growth in hot rolling, Met. Sci., 1979, Vol. 13, pp. 187 – 194.

[20] C. Zener and J. H. Hollomon, Effect of strain rate upon plastic flow of steel, J. Appl. Phys., Vol. 15, 1944, p. 22.

[21] Gleeble 1500TM, Operational Manual, Dynamic Systems Inc. US.

[22] G. E. Dieter, Mechanical Metallurgy, (1988) McGraw-Hill, New York.

[23] ASTM Specification E112 – 10 of 1982.

[24] C. A. Muojekwu, Modelling of thermomechanical and metallurgical phenomena in steel strip during hot direct rolling and run-out table of thin-cast slabs, The Univ. of British Columbia, PhD. Thesis, 1998
[25] J. L. Uvira and J. J. Jonas, Hot compression of Armco iron and silicon steel, TMS - AIME, Vol. 242, 1968, pp. 1619 – 1624.
[26] H. J. McQueen, O. Overdal, A. Cingara, and H. Gjestland, Mat. High Temp. 10 (1992), pp. 207 – 218.
[27] S. Serajzadeh and A. Karimi Taheri, An investigation on the effect of carbon and silicon on flow behaviour of steel, Material & Design, 23 (2002), pp. 271 – 276.
[28] K. Lim, P. A. Manohar, D. Lee, Y.-C. Yoo, C. M. Cady, G. T. Gray and A. D. Rollett, Constitutive modelling of high temperature mechanical behaviour of a medium C-Mn steel, MATERIALS SCIENCE FORUM; 426-432; 3903-3908 Thermec'2003 Int. conf. 4th, Processing and Manufacturing of Advanced Materials
[29] C. M. Bae, A. M. Elwazri, D. L. Lee and S. Yue, Dynamic Recrystallization behaviour in hypereutectoid steels with different carbon content, ISIJ International, Vo. 47 (2007) No. 11, pp. 1633 – 1637.
[30] C. M. Sellars and W. J. M. Tegart, La relation entre la resistance et la structure dans la deformation a chaud, Mem. Scient. Revue Metall. 63, 731 (1966)
[31] J. Sankar, D. Hawkins, and H. J. McQueen, Behaviour of low-carbon and HSLA steels during torsion-simulated continuous and interrupted hot rolling practice, Metall. Tech. 6 (1979), pp. 325 – 331.
[32] C. M. Sellars, The Physical Metallurgy of Hot Working, Keynote Address, Proc. Int. Conf. Hot Working and Forming Processes, University of Sheffield July 1979.
[33] K. Ushioda, T. Suzuki, H. Asano, and M. Tezuka, 37th MWSP Conf. Proc., ISS, Vol. XXXIII, 1996, pp. 897 – 905.
[34] D. R. Barraclough, Hot working and recrystallisation of a stainless and a low alloy steel, PhD Thesis, University of Sheffield, (1974)
[35] J. P. Hirth and L. Lothe, "Diffusive Glide and Climb Process", Theory of Dislocations , McGraw Hill, New York, (1968), pp. 484 – 530.
[36] R. Sandoström, Subgrain growth occurring by boundary migration, Acta Metall., 25, 1977, pp. 905 – 911.
[37] E. A. Brandes and G. B. Brooks (Eds.) Smithells Metals, Ref. Book, 7th Ed. Butterworth-Heinemann, Oxford, 1992. [38] K. Nohara and K Hirano, Trans. Iron Steel Inst. Japan, The Iron and Steel Institute of Japan,(1971) p. 1267.[39] H. Abe, T. Suzuki and S Okada, Trans. Japan Inst. Metals, Vol. 25, No. 4 (1984), pp. 215 – 225.
[40] G. Brauer and K. Popp, Neutron embrittlement of reactor pressure vessel steels: A challenge to Positron Annihilation and other methods, Phys. Status Solidi. B 102, (1987), pp. 79 – 90.
[41] N. I. Medvedeva, M. S. Park, D. C. van Aken and J. E. Medvedeva, "First-principles study of the Mn, Al, and C distribution and their effct on the stacking fault energies in austenite", Missouri Univ. of Sci. and Technology, Rolla, Mo 65409, Inst. Of Solid State Chem., Yekaterinburg, Russia.
[42] N. I. Medvedeva, D. C. van Aken and J. E. Medvedeva, First principles study of the Mn, Al and C distribution and their effect on the stacking fault energies in austenite, J. Phys. Cond. Matter, 23, (2011) 326003, (5pp).
[43] A. Caplain and W Chambron, Etude de l'interaction lacune–carbone dans l'alliage Ni-20% at. Fe par la méthode de l'anisotropie magnétique induite, Physica Status Solidi A, 52, (1979), pp. 299
[44] A. Caplain and W Chambron, Insuffisance du modele de lomer pour decrire l'interaction lacune-carbone dans l'alliage Ni - 20 % at. Fe Scripta Matellurgica, 11, (1977), pp. 499.
[45] R. B. McLellan, The diffusivity of lattice atoms in dilute interstitial solid solutions, Acta Metallurgica, Vol. 36, No. 8, (1988), pp. 1923 – 1928
[46] R. B. McLellan, The thermodynamics of interstitial-vacancy interactions in solid solutions, J. Phys. Chem. Solids, Vol. 49, No. 10, (1988), pp. 1213 – 1217
[47] N. I. Medvedeva, M. S. Park, D.C. Van Aken and J. E. Medvedeva, First principles study of the Mn, Al and C distribution and their effect on the stacking fault energies in FCC Fe, J. Alloys and Compounds, 582, (2014), pp. 475 – 482.

[48] C. Siyasiya and W Stumpf, Hot working of carbon-manganese strip steels: the effects of carbon and manganese content, 19th IAS Steel Conference, Rolling and Steel Products, IAS, 2013, Rosario, Santa Fe, Argentina.
[49] W Stumpf, Journal of the South African Institute of Mining and Metallurgy, Grain size modelling of a low carbon strip steel during hot rolling in a Compact Strip Production (CSP) plant using the hot charge route, Vol. 103 (2003), pp. 617 – 631
[50] Y. N. Dastur and W. C. Leslie, Metall Trans A 12 (1981) pp 749
[51] K Banks, Hot flow stress model for plain C steels under finishing mill conditions, Steel Strip Society, 8th Int. Conf. Proc. (2011), pp 181
[52] Internal communication from ArcelorMittal South Africa, Sadhana Steel Works, 2001